Appl. Phys. B 71, 907–910 (2000) / Digital Object Identifier (DOI) 10.1007/s003400000445

Applied Physics B
Lasers
and Optics

Rapid communication

First *Z*-scan n_2 measurements on crystal hosts for ultraviolet laser systems

G. Toci[1], **M. Vannini**[1], **R. Salimbeni**[1], **M.A. Dubinskii**[2], **E. Giorgetti**[3]

[1] Istituto di Elettronica Quantistica (IEQ-CNR), Via Panciatichi 56/30, 50127 Firenze, Italy
(Fax: +39-055/41-4612, E-mail: vannini@ieq.fi.cnr.it)
[2] Science & Engineering Services, Inc. 4032 Blackburn Lane, Burtonsville, MD 20866, USA
[3] Istituto di Ricerca sulle Onde Elettromagnetiche "Nello Carrara" (IROE-CNR), Via Panciatichi 64, 50127 Firenze, Italy

Received: 6 June 2000/Published online: 5 October 2000 –

Abstract. We report the results of the first measurements of the non-linear Kerr refractive index, n_2, for $LiBaF_3$ and $LiLuF_4$ crystal hosts, known as prospective UV-emitting tunable laser media when doped with Ce^{3+} ions. These n_2 values (2.7×10^{-16} and 1.5×10^{-16} cm^2/W at 532 nm, respectively), obtained using the well-established *Z*-scan technique, are important for the characterization of new optical materials particularly in relation to their potential ultrafast applications.

PACS: 42.65.-k; 42.70.Hj; 42.65.An

Laser crystals doped with Cerium (Ce^{3+}) for emission in the ultraviolet (UV) region are receiving increasing attention [1–3], because they offer an alternative way of developing an all-solid-state, tunable and efficient source of subnanosecond laser pulses, in contrast with efficient but rather complicated and expensive excimer lasers and very complicated sources based on nonlinear frequency up-conversion of tunable lasers in the red and near-infrared wavelength domains.

In this paper we report on the first (to the best of our knowledge) measurements of the nonlinear refractive index at 532 nm of two host crystals suitable for Ce^{3+} doping: $LiBaF_3$ and $LiLuF_4$. In many respects, knowledge of this parameter is imperative for the development of new laser devices, since the intensity-dependent changes of the optical parameters of the active material can strongly affect the performance of high-power laser systems. The refractive part of the nonlinearity gives rise to self-lensing, which can lead to catastrophic optical damage. Furthermore, self-phase modulation is becoming increasingly relevant in the design of ultrafast laser systems (although this possibility has yet to be demonstrated for the materials tested here).

To measure the nonlinear refractive index of these materials, we employed the sensitive and relatively simple standard *Z*-scan technique [4]. This method is based on the self-focusing, or defocusing, of an optical beam induced by a nonlinear sample, which is moved along the propagation direction (*Z* axis) of a focused beam of known spatial structure.

1 Theoretical framework

In our measurements, we used the so-called trimmed Airy beam. This beam structure is not only easier to realize than a Gaussian beam, but it also provides higher sensitivity, because the transmission variation for a given intensity in the waist is 1.5 times larger. The theory for the trimmed Airy beam, as applied to thin samples, has already been reported [5]. To correctly process our measurements, we extended this theory to the case of thick samples, because some of our crystals did not fulfil the condition $L \ll z_R$, where L is the sample length and z_R is the Rayleigh range of the beam [4].

This extension considers that, at the lowest order of approximation, a purely refracting sample of small thickness dz, placed at a distance z from the focus, determines a variation in the transmission through the on-axis aperture in the beam far field that is given by:

$$d\Delta T_{thin}(z) = kn_2^I I_0 \, dz \, F_\Psi(z/z_d) \tag{1}$$

where k is the vacuum wavenumber, I_0 is the beam intensity in the focus, n_2^I is the nonlinear refractive index, z_d is a diffraction length depending on the incident beam structure, and F_Ψ is a function of the crystal position. The overall transmission variation determined by a sample of length L is determined by properly integrating (1) over the sample length, measured in units of the beam diffraction length in the sample, $n_0 z_d$, where n_0 is the linear refractive index:

$$\Delta T_{thick}(x) = kn_2^I I_0 z_d n_0 \int_x^{x+L/(n_0 z_d)} F_\Psi(y) \, dy \tag{2}$$

where $x = z/z_d$, and z here is the distance of the sample input face from the focal plane of the unperturbed beam. This expression is a first-order approximation, because it neglects both the higher-order effects in the phase modulation originating in the individual "slice" and also the so-called

self-action, i.e. the perturbation due to the nonlinear beam refraction in the first portion of the sample, which affects the beam that crosses the remaining parts of the sample.

With a Gaussian beam, from the gaussian beam decomposition we have [4] $F_\Psi(x) = 4x/\left[(x^2+1)(x^2+9)\right]$, where $x = z/z_\mathrm{d}$, and $z_\mathrm{d} = z_\mathrm{R}$, the Rayleigh range. When applied to a Gaussian beam, (2) provides the same results already found by Hermann et al. [6] for a thick sample, at the first order in the beam intensity (see equations 28 and 29 in [6]).

For a trimmed Airy beam, the function F_Ψ can be calculated numerically using the method described by Rhee et al. [5]. In this case, $z_\mathrm{d} = (\lambda f^2)/(\pi r_\mathrm{A}^2)$, where f is the focal length of the focusing lens, and r_A is the radius of the first zero of the Airy intensity distribution at the lens plane.

Figure 1 shows the results obtained from (2) in the case of a trimmed Airy beam and for samples of different normalized lengths $L/(z_\mathrm{d}n_0)$. At this order of approximation, the curves are anti-symmetric with respect to $x = -L(2z_\mathrm{d}n_0)$. The separation of the maximum and the minimum $\Delta x_{\mathrm{p-v}}$ is about $5.3z_\mathrm{d}$ for short crystals, and it increases monotonically with the normalized crystal length, approaching the asymptotic value $\Delta x_{\mathrm{p-v}} = L/(z_\mathrm{d}n_0)$. For very long crystals, the peak-to-valley swing $\Delta T_{\mathrm{p-v}}$ saturates at a value of about

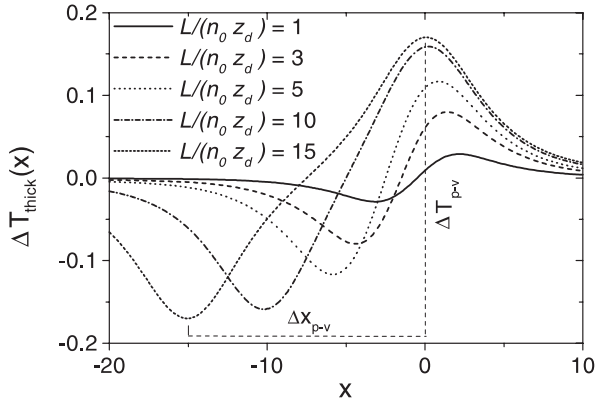

Fig. 1. Z-scan traces for increasing sample lengths, calculated from (2) for a trimmed Airy beam with $kn_2^I I_0 z_\mathrm{d} n_0 = 0.1$. The peak-to-valley amplitude $\Delta T_{\mathrm{p-v}}$ and the peak-to-valley distance $\Delta x_{\mathrm{p-v}}$ are also shown for the curve with $L/(n_0 z_\mathrm{d}) = 15$

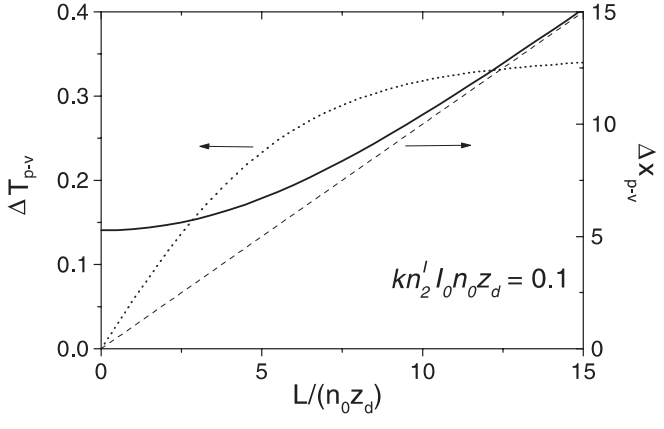

Fig. 2. Peak-to-valley swing amplitude $\Delta T_{\mathrm{p-v}}$ (*left axis*) and peak-to-valley distance $\Delta x_{\mathrm{p-v}}$ (*right axis*) for increasing normalized crystal length $L/(n_0 z_\mathrm{d})$. The *dashed straight line* shows the asymptotic behavior of the peak-to-valley separation

$3.5kn_2^I I_0 z_\mathrm{d} n_0$. Figure 2 shows the behavior of the peak-to-valley swing and the spatial separation between the maximum and the minimum as calculated from (2), for increasing normalized crystal length $L/(z_\mathrm{d}n_0)$. We found (2) to be in good agreement with the measurements which we performed on thick samples, as described in this paper.

2 Experimental set-up and data analysis

The laser that we employed to test the samples was a 10 Hz oscillator/amplifier, mode locked and frequency doubled (532 nm) Nd:YAG (EKSPLA model PL2143A). The maximum pulse energy impinging on the samples was 40 μJ, with a fluctuation < 5% (3 times the standard deviation over 100 pulses). The pulse duration was measured with the standard second-order autocorrelation method, using a 1-mm-thick BBO crystal and it had 18 ± 1 ps FWHM (assuming a sech^2 pulse shape). The trimmed Airy beam was obtained by first selecting the central part of the beam with a 400-μm-diameter pinhole, then, after 200-cm free propagation, selecting the central lobe of the resulting Airy pattern with a 6.4-mm-diameter iris, closely followed by a lens which focused the beam at a distance of 350 mm. We measured the beam structure by means of the knife-edge technique [7]. The beam radius in the focus was $w_0 = 31$ μm, with a Rayleigh range of 4.9 mm, and a beam quality factor $M^2 = 1.15$. The latter parameter is quite similar to the value resulting from the numerical simulation of a trimmed Airy beam with the same radius on the lens front plane ($M^2 = 1.06$). The peak power density in the focus was up to 145 GW/cm^2.

After the focus, the beam propagated for about 2 m and impinged on an aperture with transmission $T \approx 5\%$. The transmitted energy was measured by a silicon photodiode, whereas a beamsplitter placed between the iris and the lens sent part of the pulse energy to a second, identical photodiode, that was used as a reference. A 16-bit ADC board simultaneously acquired the two signals, which were then stored and processed on a PC. The crystal was mounted on a motorized stage with 0.1-μm resolution, controlled by the same PC. For each crystal position along the scan range, we measured and averaged over several laser pulses (typically 35) the time-averaged aperture transmission $\langle T \rangle = E_{\mathrm{aperture}}/E_{\mathrm{total}}$. For each sample, we acquired several Z-scan traces at various input pulse energies, modulated with rotating disk variable attenuators. The fluctuations in the linear transmission of the sample were compensated for by complementing each scan with one at a low pulse energy and by calculating their ratio. The overall sensitivity in the transmission variation thus achieved ranged from 1% for the samples with better optical quality to 1.8% for the worst ones. Figure 3 shows two typical Z-scan traces, obtained with a $LiBaF_3$ sample and with the sapphire sample used for calibration, after subtraction of the linear transmission.

We determined the n_2^I coefficient by means of relative measurements with respect to a 5-mm-long sapphire (Al_2O_3) sample, because the n_2^I of sapphire has been accurately determined by means of several methods, including the Z-scan at 532 nm [8]. Relative measurements are convenient when using a laser source, the spatial and, particularly, the tempo-

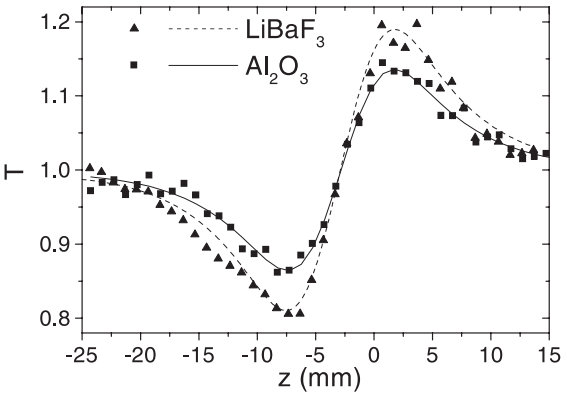

Fig. 3. *Z*-scan measurement obtained after subtraction of the linear transmission fluctuations with a 9-mm-long $LiBaF_3$ sample, $10.0 \pm 0.3\,\mu J$ pulse energy (*triangles*) and with a 5-mm-long sapphire sample, 9.08 ± 0.7 pulse energy (*squares*), used for calibration. The *solid* and *dashed lines* are the best fits of (3), with $C = 0.272 \pm 0.004$ and $C = 0.202 \pm 0.007$, respectively

ral parameters of which are difficult to determine accurately, as happens in the picosecond or femtosecond pulse regimes.

The accurate method for relative *Z*-scan measurements with arbitrary beam structure and pulse shape described by Bridges et al. [9], which is based on a careful matching between the lengths of test and reference samples, is not useful in our situation, because of the reduced number of available samples. We therefore used the following method, which requires knowledge of the beam structure.

Each series of measurements on an unknown sample was closely preceded or followed by a calibration scan with the sapphire sample, to minimize the effects of possible drifts in the laser emission parameters. After correction for the linear transmission, we fitted each *Z*-scan profile using (2), modified for the time-averaged transmission, in the form:

$$\langle \Delta T_{\text{thick}}(x) \rangle = C \int_{x}^{x+L/(n_0 z_d)} F_\Psi(y)\,\mathrm{d}y \tag{3}$$

where C corresponds to

$$C = k n_0 n_2^I z_d (2/\pi w^2) \left[\int f(t)^2\,\mathrm{d}t \Big/ \int f(t)\,\mathrm{d}t \right] E'_p \tag{4}$$

where: E'_p, pulse energy (corrected for the Fresnel losses); $f(t)$ pulse temporal shape [such that $f(t)E'_p = P(t)$, instantaneous power]; and w, effective beam radius in the focus [such that the focal power density is $I(t) = P(t)2/\pi w^2$]. For each series of measurements taken on a given sample at different energy levels, we then calculated the energy slopes b defined using $C(E'_p) = bE'_p$ and, lastly, the n_2^I value of the sample given by

$$n_{2\,\text{Sam}}^I = \left[b_{\text{Sam}} n_{0\,\text{Ref}} n_{2\,\text{Ref}}^I \right] / \left[b_{\text{Ref}} n_{0\,\text{Sam}} \right] \tag{5}$$

The subscripts Sam and Ref indicate the sample and the reference materials, respectively.

According to our experimental situation, in the evaluation of the integral in (3) for the fittings we used the function $F_\Psi(x)$ valid for the trimmed Airy beam. This was necessary because the dependence of the function $\langle \Delta T_{\text{thick}}(x) \rangle$ on the crystal length is a characteristic of the actual beam structure. The use of an improper beam structure (i.e. a Gaussian beam instead of the trimmed Airy beam) would therefore introduce a systematic error when comparing reference and sample crystals of different optical lengths. The thick-sample theory was also used to process the measurements obtained with the thin $LiLuF_4$ sample, because they were calibrated with a thick sapphire reference.

3 Results and conclusions

Table 1 reports the values obtained as described above. In addition to the previously uncharacterized materials, i.e. $LiLuF_4$ and $LiBaF_3$, we also report the measurements obtained on a LiCAF sample and on a fused-silica sample. The n_2^I value for LiCAF was measured because, although this host appears in the literature as a suitable material for Ce^{3+} doping for UV laser emission, only the value at 1064 nm is available [10]. It is reasonable to expect that this value of n_2^I will increase at shorter wavelengths. The fused silica is a fairly well-characterized material, and the good agreement between the value reported here and the existing references [8] provides good validation for the measurement set-up and the data-processing technique that we adopted. The error reported in the $n_2^I(\text{sample})/n_2^I(Al_2O_3)$ ratio depends on the statistical error of the fits and on the determination of the energy slopes, whereas the errors in the absolute values of n_2^I also account for the error in the reported value of sapphire n_2^I. According to Table 1, all the materials exhibit a n_2^I value smaller than that of Al_2O_3. We did not observe any two-photons absorption effects within our sinsitivity limits of 1% in the variation of the transmission.

In conclusion, this paper reports the first (to the best of our knowledge) measurements of the n_2^I nonlinearity obtained by using the *Z*-scan technique for important UV host crystals such as $LiBaF_3$ and $LiLuF_4$. Our interest in this work was stimulated by previous $LiBaF_3$ and $LiLuF_4$ investigations, which were aimed at the characterization of these crystals with Ce^{3+}-doping for an all-solid-state UV laser. The n_2^I

Table 1. Experimental results

Sample	L (mm)	n_0	$\frac{n_2^I}{n_2^I(Al_2O_3)}$	Measured n_2^I (10^{-16} cm^2/W)	Reported n_2^I (10^{-16} cm^2/W)	Ref.
Al_2O_3	5.0	1.76	–	–	3.3 ± 0.7	8
$LiBaF_3$	9.0	1.544	0.82 ± 0.14	2.7 ± 0.9	–	
$LiLuF_4$	1.0	1.47	0.45 ± 0.04	1.5 ± 0.5	–	
SiO_2	7.6	1.48	0.64 ± 0.07	2.1 ± 0.6	2.2 ± 0.45	8
LiCAF	12.6	1.398	0.16 ± 0.02	0.73 ± 0.25	0.4 (1064 nm)	10

value at 532 nm was also measured for LiCAF: it was larger than the previously reported one obtained at 1064 nm, evidence of the expected wavelength dispersion of this parameter. The measurement of the n_2^I value of the above materials at shorter wavelengths, closer to the lasing wavelength associated with Ce^{3+}-activation, will be the subject of future work.

References

1. Z. Liu, N. Sarukura, M.A. Dubinskii, R.Y. Abdulsabirov, S.L. Korableva: J. Nonl. Opt. Phys. Mat. **8**, 41 (1999)
2. M.A. Dubinskii, K.L. Schepler, R.Y. Abduslabirov, Sl.L. Korableva: J. Mod. Opt. **45**, 1993 (1998)
3. N. Sarukura, M.A. Dubinskii, Z. Liu, V.V. Semansko, A.K. Naumov, S.L. Korableva, R.Y. Abdulsabirov, K. Edamatsu, Y. Suzuki, T. Ito, Y. Segawa: IEEE J. Sel. Top. Quantum Electron. **1**, 792 (1995)
4. M. Sheik-Bahae, A.A. Said, T.H. Wei, D.J. Hagan, E.W. Van Stryland: IEEE J. Quantum Electron. **QE-26**, 760 (1990)
5. B.K. Rhee, J.S. Byun, E.W. Van Stryland: J. Opt. Soc. Am. B **13**, 2720 (1996)
6. J.A. Herrmann, R.G. McDuff: J. Opt. Soc. Am. B **10**, 2056 (1993)
7. A.E. Siegman, M.W. Sasnett, T.F. Johnston: IEEE J. Quantum Electron. **QE-27**, 1098 (1991)
8. R. DeSalvo, A.A. Said, D.J. Hagan, E.W. Van Stryland, M. Sheik-Bahae: IEEE J. Quantum Electron. **QE-32**, 1324 (1996)
9. R.E. Bridges, G.L. Fischer, R.W. Boyd: Opt. Lett. **20**, 1821 (1995)
10. P. Beaud, M.C. Richardson, Y.F. Chen, B.H.T. Chai: IEEE J. Quantum Electron. **QE-30**, 1259 (1994)